

1

## 2 **Supplementary Information for**

### 3 **Quantifying the effectiveness of betaherpesvirus-vectored transmissible vaccines**

4 **Tanner J. Varrelman, Christopher H. Remien, Andrew J. Basinski, Shelley Gorman, Alec Redwood and Scott L. Nuismer**

5 **Tanner J. Varrelman.**

6 **E-mail: [varr3316@vandals.uidaho.edu](mailto:varr3316@vandals.uidaho.edu)**

#### 7 **This PDF file includes:**

8     Supplementary text

9     Figs. S1 to S4 (not allowed for Brief Reports)

10    Tables S1 to S3 (not allowed for Brief Reports)

11    SI References

## 12 Supporting Information Text

13 This section provides further details on the methods used to evaluate the effectiveness of an MCMV-vectored transmissible  
 14 vaccine. To this end, we: 1) detail the stochastic model that was used for the Approximate Bayesian Computation (ABC)  
 15 process, 2) provide further details regarding the ABC algorithm itself, 3) detail the steady-state solutions to our model that  
 16 give rise to the vaccine and pathogen basic reproductive numbers, and 4) develop and analyze models of partial vaccine efficacy.

## 17 Stochastic Epidemiological Model of MCMV for ABC

18 To estimate the epidemiological parameters of MCMV from the time-series data set, we implement a continuous-time Markov  
 19 chain (CTMC) version of the model described in the main text Eq. (3)–Eq. (5), with some small modifications to the base  
 20 model. Briefly, the CTMC version of our model is a stochastic process where the state variables are discrete random variables  
 21 and the time scale is continuous (1). For this implementation of the model, the birth and death rates were set to zero because of  
 22 the relatively constant population size of the founder population observed by Farroway et al. (2002) (2). Further, we include an  
 23 additional exposed class ( $E_2$ ) to account for the initial fraction of the population that was exposed to MCMV via IP injection.  
 24 We include the additional exposed class because exposure via transmission and IP injection are biologically different. With  
 25 the addition of the IP injected class ( $E_2$ ), we introduce another parameter,  $\sigma_2$ , which defines the rate at which IP injected  
 26 individuals become infectious. We simulate the model using the Gillespie algorithm (3). Events, transitions, and transition  
 27 rates are given in Table S1.

Event	Transition	Transition Rate
Susceptible infected with MCMV	$S \rightarrow S - 1, E_1 \rightarrow E_1 + 1$	$\frac{\beta_v I}{N}$
Exposed via transmission becomes infectious	$E_1 \rightarrow E_1 - 1, I \rightarrow I + 1$	$\sigma$
Exposed via IP injection becomes infectious	$E_2 \rightarrow E_2 - 1, I \rightarrow I + 1$	$\sigma_2$

Table S1. The events, transitions, and transition rates found in the CTMC model.

## 28 Approximate Bayesian Computation

29 We use Approximate Bayesian Computation in combination with the time-series data set described by Farroway et al. (2002)  
 30 to produce baseline parameter estimates for MCMV. We begin the ABC process by taking a random sample of the parameter  
 31 values from the prior distributions (described in Table S2). These priors were informed by values reported within the MCMV  
 32 literature. These parameter samples are then fed into the CTMC model, and a sample trajectory is generated using the  
 33 Gillespie algorithm. Model simulations were initiated according to the initial conditions described in Farroway et al. (2002)  
 34 ( $S = 16, E_1 = 0, E_2 = 6, I = 0$ ). We stop the simulations once the time in the model has reached 84 days (the last time  
 35 step described in Farroway et al. (2002)), and we take a binomial sample of the number of infectious individuals at each time  
 36 point detailed in the data set, according to the sampling effort for a given rodent enclosure. We take a binomial sample at  
 37 each time point in an attempt to recreate the possibility for sampling error in the MCMV transmission experiments. The  
 38 binomial distribution is chosen for our sampling, as an individual is either MCMV positive (1) or negative (0) at each time  
 39 point. We then calculate the residual sum of squares for our simulated sample across all enclosures at a given time point, and  
 40 then averaged the value across all time points. The resulting quantity is a measure of how well the parameter samples and  
 41 simulated model perform against the actual transmission experiments. If this value was less than or equal to our acceptance  
 42 criteria (0.1), then the parameters for that simulated run were added to the multivariate posterior distribution. The ABC  
 43 process was carried out until the multivariate posterior distribution accumulated twenty-five thousand samples.

Parameter	Prior	Justification
$\beta$	Uniform on [0.0005, 0.009]	The range was determined based on values that could plausibly lead to the observed seroprevalence.
$\sigma$	Gamma with mean 0.099 and shape 75	The mode was selected based on known MCMV seroconversion (4).
$\sigma_2$	Gamma with mean 0.099 and shape 100	The mode was selected based on the seroconversion of MCMV injected via IP injection (4).

Table S2. Prior distributions for each parameter in the MCMV model.

## 44 Steady-state model solutions

45 To find steady-state solutions of Eq. (7)–Eq. (11) in the main text, we set the left hand side of the equations to zero and solved  
46 the resulting algebraic equations for each of the state variables. This yields three steady-state solutions. The first,

$$47 \quad S = \frac{b(d + \sigma)}{\sigma\beta_v} \quad [1]$$

$$48 \quad E = \frac{-bd^2 - bd\sigma + b\sigma\beta_v}{\sigma(d + \sigma)\beta_v} \quad [2]$$

$$49 \quad I = \frac{-bd^2 - bd\sigma + b\sigma\beta_v}{d(d + \sigma)\beta_v} \quad [3]$$

$$50 \quad P = 0 \quad [4]$$

$$51 \quad R = 0, \quad [5]$$

52 the second,

$$54 \quad S = \frac{b(d + \delta)}{d\beta_p} \quad [6]$$

$$55 \quad E = 0 \quad [7]$$

$$56 \quad I = 0 \quad [8]$$

$$57 \quad P = \frac{-bd - b\delta + b\beta_p}{(d + \delta)\beta_p} \quad [9]$$

$$58 \quad R = -\frac{b\delta(d + \delta - \beta_p)}{d(d + \delta)\beta_p}, \quad [10]$$

59 and the third,

$$61 \quad S = \frac{b}{d} \quad [11]$$

$$62 \quad E = 0 \quad [12]$$

$$63 \quad I = 0 \quad [13]$$

$$64 \quad P = 0 \quad [14]$$

$$65 \quad R = 0. \quad [15]$$

66 From these solutions, we see that there are three possible scenarios, 1) the vaccine is endemic and the pathogen is absent, 2)  
67 the pathogen is present and the vaccine is absent, and 3) both the pathogen and vaccine are absent from the population.

## 68 Calculating basic reproductive numbers

69 To find the analytical solution for the basic reproductive number of MCMV and the pathogen, we performed a standard  
70 stability analysis on the infection-free steady state. To perform this analysis, we linearized the system of differential equations  
71 Eq. (7)–Eq. (11) in the main text, and evaluated the resulting Jacobian matrix at the equilibrium solution (Eq. (11)–Eq. (15)).  
72 We then found the eigenvalues of the resulting matrix. From these eigenvalues, we were able to find the threshold transmission  
73 conditions that lead to instability of the infection-free steady state:  
74

$$75 \quad R_{0,v} \equiv \frac{\beta_v\sigma}{d(d + \sigma)} > 1, \quad [16]$$

76 or

$$77 \quad R_{0,p} \equiv \frac{\beta_p}{d + \delta} > 1. \quad [17]$$

78 According to the classic definition of  $R_0$ , the quantity defined by Eq. (16) is MCMV's reproductive number. Similarly, Eq. (17)  
79 represents the reproductive number of the pathogen.

80 For completeness, we performed a stability analysis on the MCMV-endemic steady state (Eq. (1)–Eq. (5)) and the  
81 pathogen-endemic steady state (Eq. (6)–Eq. (10)). We found that the vaccine-endemic steady state is stable if  
82

$$83 \quad R_{0,v} > 1, \quad [18]$$

84 and

$$85 \quad R_{0,v} > R_{0,p}. \quad [19]$$

86 Further, we find that the pathogen-endemic steady state is stable if

$$87 \quad R_{0,p} > 1, \quad [20]$$

88 and

$$89 \quad R_{0,p} > R_{0,v}. \quad [21]$$

95 **Partial vaccine efficacy: imperfect transmission blocking**

96 To account for partial vaccine efficacy, we extend the model described in the main text Eq. (7)–Eq. (11) to cases where  
 97 co-infection between the transmissible vaccine and the pathogen reduces—but does not completely block—pathogen transmission.  
 98 In this model, individuals that have been exposed to the vaccine ( $E$ ), as well as those that are actively infectious with the vaccine  
 99 ( $I$ ), can be infected by the target pathogen. In these cases, individuals transition into the vaccine-exposed pathogen-infected  
 100 class ( $E_p$ ), and the vaccine-infectious pathogen-infected class ( $I_p$ ). From these co-infected classes, pathogen transmission is  
 101 reduced by a factor of ( $\rho$ ). Further, individuals in the  $E_p$  and  $I_p$  classes can recover from pathogen infection and transition into  
 102 the  $E_r$  and  $I_r$  classes, respectively. Moreover, all individuals that have been exposed to the vaccine ( $E$ ,  $E_p$ , and  $E_r$ ), transition  
 103 into their corresponding vaccine infectious class at rate  $\sigma$ . When  $\rho = 1$ , the vaccine perfectly blocks pathogen transmission and  
 104 the co-infection model reduces to equations Eq. (7)–Eq. (11) in the main text. All model parameters are described in the main  
 105 text (i.e.,  $\beta_v$ ,  $\sigma$ ,  $\beta_p$ ,  $\delta$ ,  $b$ ,  $d$ ). These assumptions lead to the following extended model of co-infection:

$$106 \quad \frac{dS}{dt} = b - S \left( \frac{\beta_p P + (1 - \rho)\beta_p(E_p + I_p) + \beta_v(I + I_p + I_r)}{N} + d \right) \quad [22]$$

$$107 \quad \frac{dE}{dt} = S \left( \frac{\beta_v(I + I_p + I_r)}{N} \right) - E \left( \frac{\beta_p P + (1 - \rho)\beta_p(E_p + I_p)}{N} + \sigma + d \right) \quad [23]$$

$$108 \quad \frac{dE_p}{dt} = E \left( \frac{\beta_p P + (1 - \rho)\beta_p(E_p + I_p)}{N} \right) - E_p(\sigma + \delta + d) \quad [24]$$

$$109 \quad \frac{dE_r}{dt} = \delta E_p - E_r(\sigma + d) \quad [25]$$

$$110 \quad \frac{dI}{dt} = \sigma E - I \left( \frac{\beta_p P + (1 - \rho)\beta_p(E_p + I_p)}{N} + d \right) \quad [26]$$

$$111 \quad \frac{dI_p}{dt} = I \left( \frac{\beta_p P + (1 - \rho)\beta_p(E_p + I_p)}{N} \right) + \sigma E_p - I_p(\delta + d) \quad [27]$$

$$112 \quad \frac{dI_r}{dt} = \delta I_p + \sigma E_r - dI_r \quad [28]$$

$$113 \quad \frac{dP}{dt} = S \left( \frac{\beta_p P + (1 - \rho)\beta_p(E_p + I_p)}{N} \right) - P(\delta + d) \quad [29]$$

$$114 \quad \frac{dR}{dt} = \delta P - dR. \quad [30]$$

116 Simulating this model against endemic LASV and LCMV yielded Fig. 4 in the main text. For these simulations, we define  
 117 pathogen prevalence as the fraction of individuals that actively transmit the pathogen ( $E_p(1 - \rho) + I_p(1 - \rho) + P$ )/ $N$ .

118 **Critical vaccine efficacy.** To solve for the critical vaccine efficacy that must be achieved for a transmissible vaccine to protect a  
 119 reservoir population from pathogen invasion, we linearized the pathogen-infected subsystem ( $E_p$ ,  $I_p$ ,  $P$ ) (Eq. (24), Eq. (27),  
 120 Eq. (29)) about the pathogen-free steady state. We then solved for the vaccine efficacy ( $\rho$ ) that leads to a positive eigenvalue  
 121 of the Jacobian matrix of this linearized subsystem. To determine if this condition for pathogen protection also guarantees  
 122 elimination of an endemic pathogen, we simulated the partial efficacy model starting at the pathogen-endemic steady state. We  
 123 introduced the transmissible vaccine to 10% of the susceptible population, with a range of vaccine efficacies and potential  
 124 pathogen  $R_0$ 's. We find that over the range of pathogen  $R_0$ 's we considered, the critical vaccine efficacy for eliminating an  
 125 endemic pathogen is equivalent to the efficacy required to prevent pathogen invasion.

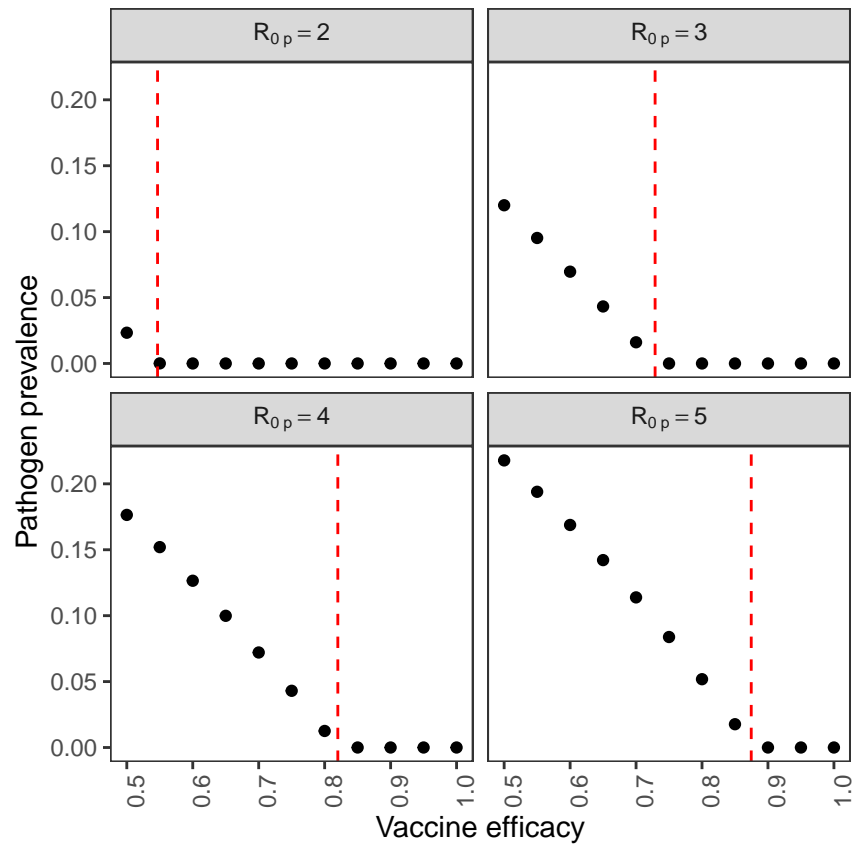


**Fig. S1.** Pathogen prevalence with varying levels of vaccine efficacy across a range of pathogen  $R_0$ 's. Simulations were initialized at the endemic pathogen steady state, with 10% of the susceptible population removed and exposed to the transmissible vaccine. Simulations were carried out for a duration of 10,000 days, with the pathogen prevalence being recorded at the final time point. The parameters used to perform these simulations are as follows:  $\beta_v = 0.033 \text{ individual}^{-1} \text{ day}^{-1}$ ,  $\sigma = 0.099 \text{ day}^{-1}$ ,  $d = 0.00274 \text{ day}^{-1}$ ,  $b = 1.37 \text{ day}^{-1}$ .

126 **Varying vaccination rate.** To demonstrate the impact of varying the initial fraction of susceptible hosts that are vaccinated,  
 127 we provide a complementary figure to Fig. 3 in the main text. Here, we expose 1% of the susceptible population to the  
 128 transmissible vaccine, and find that the average time required to reduce the prevalence of LASV and LCMV by 95% increased  
 129 by 137 and 101 days, respectively (Fig. S2).

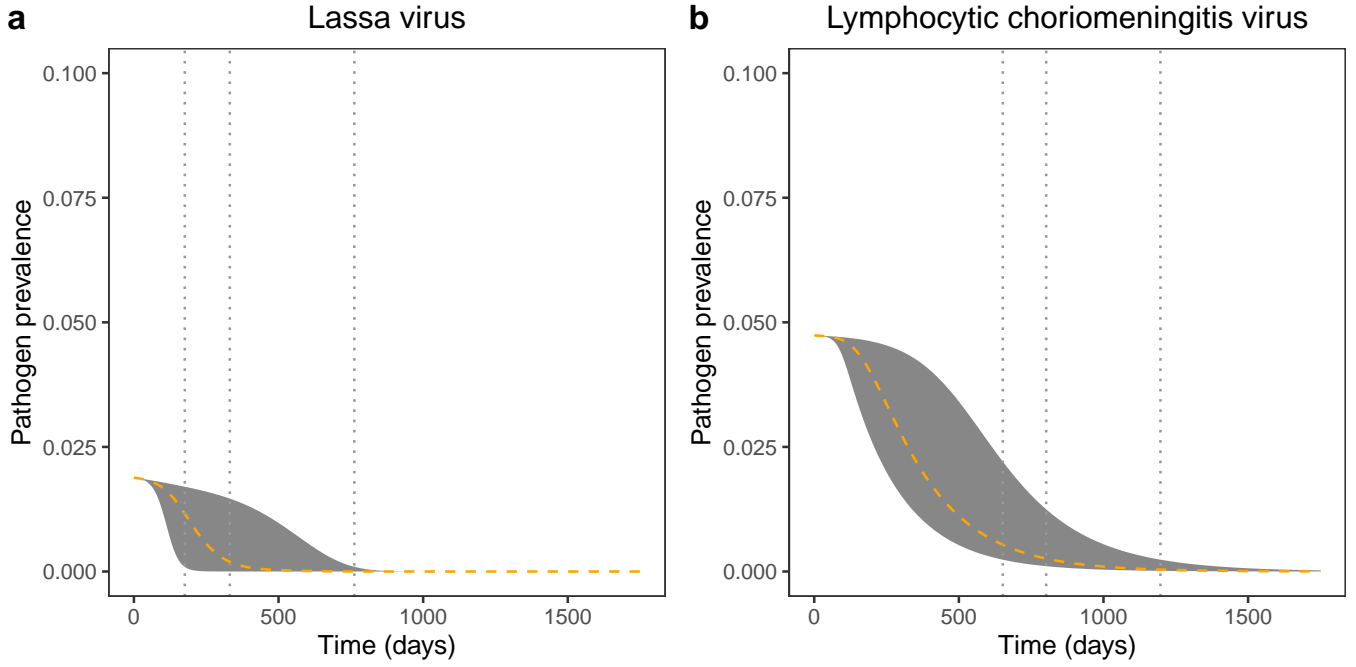


**Fig. S2.** Temporal dynamics of (a) Lassa virus (LASV) and (b) Lymphocytic Choriomeningitis virus (LCMV) reduction as a result of using a MCMV-vectored transmissible vaccine. Simulations are initialized at the steady state quantities for susceptible and pathogen infected individuals, with 1% of the susceptible population exposed to the transmissible vaccine. For each pathogen we randomly sampled  $\beta_v$  and  $\sigma$  from the posterior distribution 100 times, and simulated our model forward in time for each set of parameters. The gray region represents the range of values observed across the 100 replicate simulations, where the orange dashed line is the mean. The gray vertical lines indicate the minimum, mean, and maximum time to 95% pathogen reduction ((a) min=176 days, mean=331.45 days, max=762 days (b) min=652 days, mean=801.98 days, max=1197 days).

### Partial vaccine efficacy: imperfect infection blocking

To consider scenarios where the transmissible vaccine is imperfect with respect to blocking infection by the pathogen (rather than transmission), we formulated an additional model of partial vaccine efficacy. This model uses the same notation as the previous model of partial vaccine efficacy, but  $\rho$  now indicates the reduction in pathogen infection rate experienced by vaccine exposed and vaccine infected classes. The resulting model is as follows:

$$\frac{dS}{dt} = b - S \left( \frac{\beta_p(P + E_p + I_p) + \beta_v(I + I_p + I_r)}{N} + d \right) \quad [31]$$

$$\frac{dE}{dt} = \frac{\beta_v S(I + I_p + I_r)}{N} - E \left( \frac{(1 - \rho)\beta_p(P + E_p + I_p)}{N} + \sigma + d \right) \quad [32]$$

$$\frac{dE_p}{dt} = \frac{(1 - \rho)\beta_p E(P + E_p + I_p)}{N} - (\sigma + \delta + d)E_p \quad [33]$$

$$\frac{dE_r}{dt} = \delta E_p - (\sigma + d)E_r \quad [34]$$

$$\frac{dI}{dt} = \sigma E - \frac{(1 - \rho)\beta_p I(P + E_p + I_p)}{N} - dI \quad [35]$$

$$\frac{dI_p}{dt} = \sigma E_p + \frac{(1 - \rho)\beta_p I(P + E_p + I_p)}{N} - (\delta + d)I_p \quad [36]$$

$$\frac{dI_r}{dt} = \delta I_p + \sigma E_r - dI_r \quad [37]$$

$$\frac{dP}{dt} = \frac{\beta_p S(P + E_p + I_p)}{N} - (\delta + d)P \quad [38]$$

$$\frac{dR}{dt} = \delta P - dR \quad [39]$$

$$\quad \quad \quad [40]$$

Recreating Fig. 4 from the main text, we find that changing the formulation of partial efficacy from transmission blocking to infection blocking increases the time required to reduce the prevalence of an endemic pathogen. Specifically, we find that when vaccine efficacy is 50%, the time to reduce the prevalence of LASV and LCMV by 95% is increased by 6 and 19 days, respectively, relative to a partially effective transmission blocking vaccine (Fig. S3).

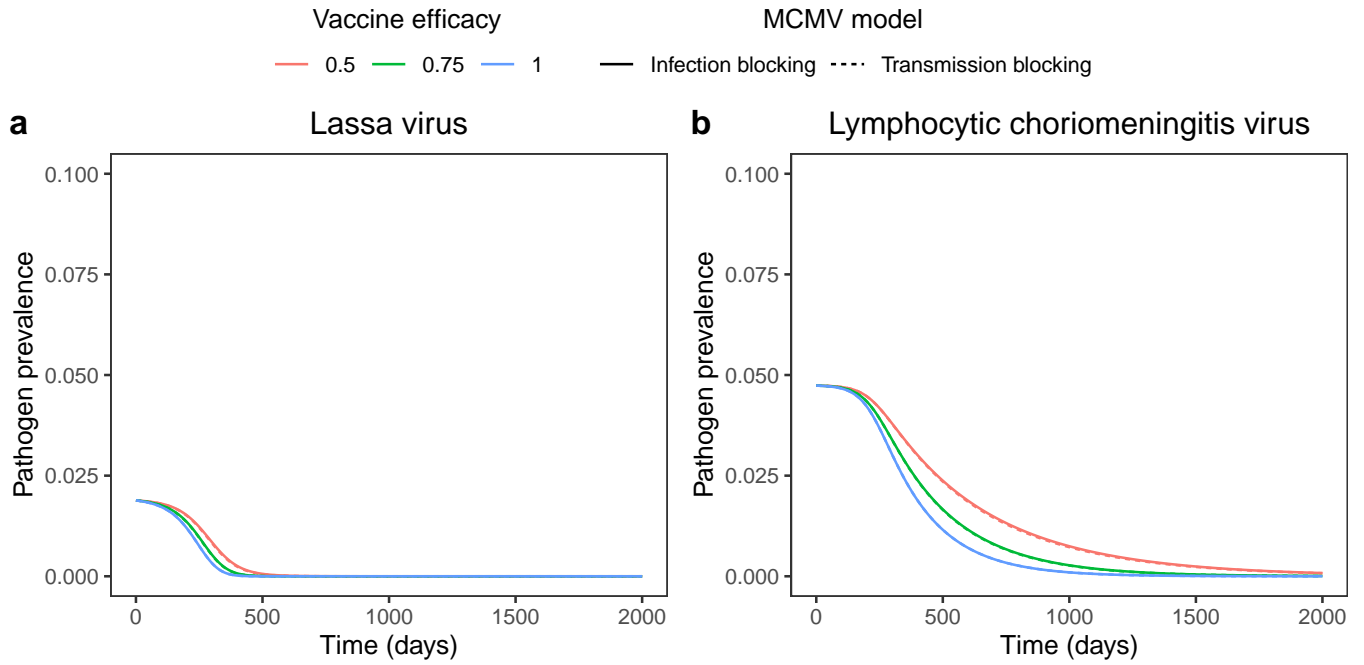


**Fig. S3.** Temporal dynamics of (a) Lassa virus (LASV) and (b) Lymphocytic Choriomeningitis virus (LCMV) reduction as a result of using an MCMV-vectored transmissible vaccine with varying levels of efficacy. Here, the vaccine blocks or partially blocks pathogen infection (solid lines) rather than transmission as in the results reported in Fig. 4 of the main text (dashed lines). Simulations are initialized at the steady state quantities for susceptible and pathogen infected individuals, where 10% of the susceptible population is exposed to the transmissible vaccine. The parameters used to perform these simulations are as followed:  $\beta_v = 0.033 \text{ individual}^{-1} \text{ day}^{-1}$ ,  $\sigma = 0.099 \text{ day}^{-1}$ ,  $d = 0.00274 \text{ day}^{-1}$ ,  $b = 1.37 \text{ day}^{-1}$ .

### 150 Delayed pathogen immunity

151 The mathematical model described in the main text assumes that individuals exposed to the transmissible vaccine are instantly  
 152 immune to pathogen infection. In reality, the process of gaining protective immunity through vaccination is not an instantaneous  
 153 process. Here, we relax this assumption and allow vaccine exposed individuals to be infected with the target pathogen. These  
 154 vaccine exposed individuals do not gain protective immunity to the pathogen until they transition into the vaccine infectious  
 155 class. Using the same parameter and state variable notation as described previously, these assumptions lead to following system  
 156 of differential equations:

$$157 \quad \frac{dS}{dt} = b - S \left( \frac{\beta_p(P + E_p) + \beta_v(I + I_p + I_r)}{N} + d \right) \quad [41]$$

$$158 \quad \frac{dE}{dt} = S \left( \frac{\beta_v(I + I_p + I_r)}{N} \right) - E \left( \frac{\beta_p(P + E_p)}{N} + \sigma + d \right) \quad [42]$$

$$159 \quad \frac{dE_p}{dt} = E \left( \frac{\beta_p(P + E_p)}{N} \right) - E_p(\sigma + \delta + d) \quad [43]$$

$$160 \quad \frac{dE_r}{dt} = \delta E_p - E_r(\sigma + d) \quad [44]$$

$$161 \quad \frac{dI}{dt} = \sigma E - dI \quad [45]$$

$$162 \quad \frac{dI_p}{dt} = \sigma E_p - I_p(\delta + d) \quad [46]$$

$$163 \quad \frac{dI_r}{dt} = \delta I_p + \sigma E_r - dI_r \quad [47]$$

$$164 \quad \frac{dP}{dt} = S \left( \frac{\beta_p(P + E_p)}{N} \right) - P(\delta + d) \quad [48]$$

$$165 \quad \frac{dR}{dt} = \delta P - dR. \quad [49]$$

167 Simulating pathogen reduction with this delayed immunity model and comparing the results to the immediate immunity model  
 168 from the main text reveals that delayed immunity has minimal impact on a transmissible vaccine's ability to reduce an endemic  
 169 pathogen. Specifically, we find that delayed immunity increases the time required to reduce the prevalence of LASV and LCMV  
 170 by 95% by only 6 and 20 days, respectively.

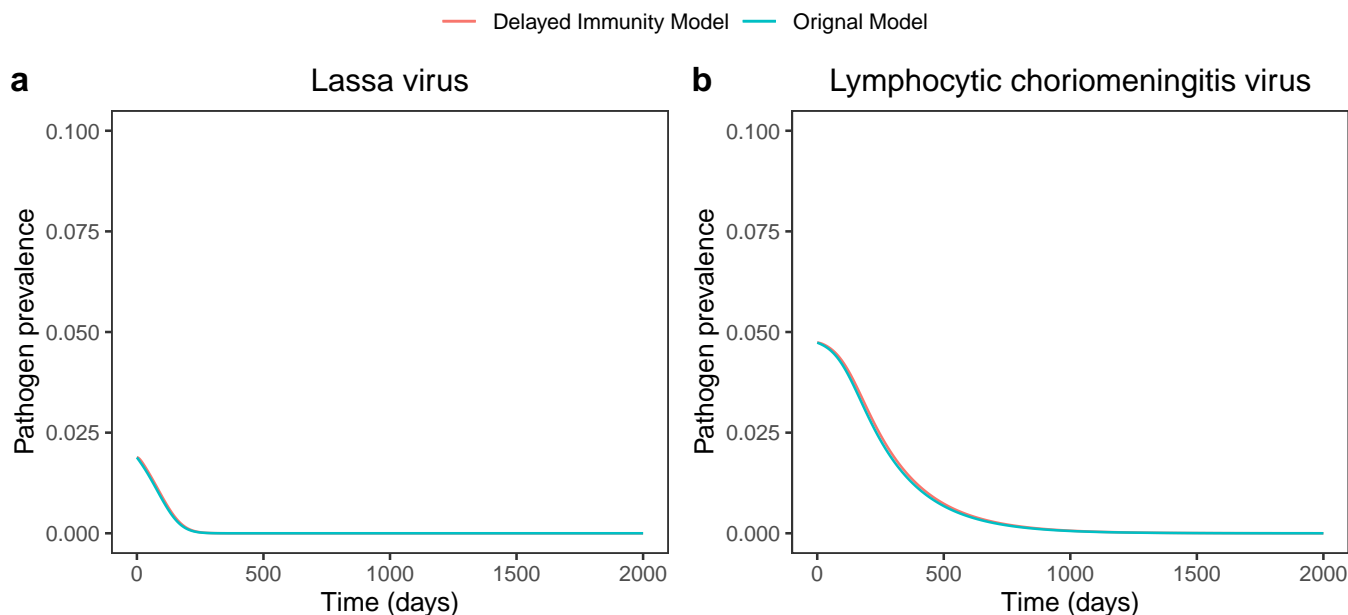


**Fig. S4.** Temporal dynamics of (a) Lassa virus (LASV) and (b) Lymphocytic Choriomeningitis virus (LCMV) reduction as a result of using an MCMV-vectored transmissible vaccine. Simulations are initialized at the steady state quantities for susceptible and pathogen infected individuals, where 10% of the susceptible population is exposed to the transmissible vaccine. Here we compare the model in the main text to the delayed pathogen immunity model described above.

171 **Prevalence of MCMV in Australian locations**

Location	Strain	Number Tested	Number Positive	Prevalence	Prevalence: Lower CI	Prevalence: Upper CI
Boullanger Island	G4	27	11	0.407	0.224	0.612
Macquarie Island	G4	40	40	1	0.912	1
Canberra	G4	12	9	0.75	0.428	0.945
Walpeup	G4	38	22	0.579	0.408	0.737
Boullanger Island	K181	27	27	1	0.872	1
Macquarie Island	K181	40	11	0.275	0.146	0.439
Canberra	K181	12	11	0.917	0.615	0.998
Walpeup	K181	38	21	0.552	0.383	0.714

**Table S3.** Sampling intensity across the various sites described in Gorman et al. (2006). Clopper-Pearson 95% intervals were calculated for each prevalence in an attempt to account for sampling error.

172 **References**

173 1. LJ Allen, An introduction to stochastic epidemic models in *Mathematical Epidemiology*, eds. F Brauer, J Wu, P van den  
174 Driessche. (Springer), pp. 93–94 (2008).  
175 2. LN Farroway, G Singleton, MA Lawson, DA Jones, The impact of murine cytomegalovirus (mcmv) on enclosure populations  
176 of house mice (*Mus domesticus*). *Wildl. Res.* **29**, 11–17 (2002).  
177 3. DT Gillespie, A general method for numerically simulating the stochastic time evolution of coupled chemical reactions. *J.*  
178 *Comput. Phys.* **22**, 403–434 (1976).  
179 4. AR McWhorter, et al., Natural killer cell dependent within-host competition arises during multiple mcmv infection:  
180 Consequences for viral transmission and evolution. *PLOS Pathog.* **9**, 1–13 (2013).